Position-dependency of Fuel Pin Homogenization in a Pressurized Water Reactor

Woong Heo and Yonghee Kim*
Korea Advanced Institute of Science and Technolgy (KAIST), 291 Daehak-ro, Yuseong-gu, Daejeon, Korea, 34141
**Corresponding author: yongheekim@kaist.ac.kr*

1. Introduction

There are efforts under way to develop a high fidelity multi-physics core analysis system which integrates the analyses of neutronics, thermal-hydraulic, fuel structural mechanics, and fuel performance with the current advancement of computer technology. By considering the multi-physics effects more comprehensively, it is possible to acquire precise local parameters which can result in a more accurate core design and safety assessment.

A conventional approach of the multi-physics neutronics calculation for the pressurized water reactor (PWR) is to apply nodal methods. Since the nodal methods are basically based on the use of assembly-wise homogenized parameters, additional pin power reconstruction processes are necessary to obtain local power information. In the past, pin-by-pin core calculation was impractical due to the limited computational hardware capability. With the rapid advancement of computer technology, it is now perhaps quite practical to perform the direct pin-by-pin core calculation. As such, fully heterogeneous transport solvers based on both stochastic and deterministic methods have been developed for the acquisition of exact local parameters. However, the 3-D transport reactor analysis is still challenging because of the very high computational requirement.

Alternative options are to apply multi-group lower-order transport methods (e.g. SP_N) or diffusion methods on the pin-by-pin core calculations. If group correction factors (which must be used to complement the disadvantages caused the by lower-order methods and pin environment effect approximations) are used, it is expected that fast pin-wise calculations may be possible with transport-comparable accuracy. Thereby, pin-by-pin core analyses based on the multi-group diffusion or lower order transport method have been studied quite recently [1, 2].

There are several very well-known and verified methods to generate the pin-level correction factors, such as generalized equivalence theory (GET) [3] and super-homogenization (SPH) [4]. Therefore, rather than discussing the method to obtain the pin-level correction factors itself, this study instead rigorously investigates effects of the pin environment on the homogenized cross sections of the pins. This study can be used to provide a baseline data for the pin-level core analysis.

2. Methods and Results

2.1 Reactor Core Model and Calculation

A modified 2-D EPRI-9 benchmark model [5] was chosen as the reference core in this study. Two modifications are made: (1) the benchmark model consists of 17x17 fuel assembly lattice based on Westinghouse's AP1000 design [6], and (2) inter-assembly gap was not modeled to simplify the problem. Figure 1 depicts radial view of the benchmark problem. Note that assemblies numbered 1 to 4 are the four target assemblies in the 2-group constant comparisons. There are two different types of fuel assemblies in the problem, which differ mainly in terms of its UO_2 enrichment content: FA-1 consists of 3.0 w/o UO_2 while FA-2 consists of 4.9 w/o UO_2 fuels. Figure 2 illustrates the fuel assembly modeled in this work with target pin cells labeled T1~T21, G, R1~R2 for the 2-group constant comparisons. Detailed material and temperature information are listed in Table I.

The Monte Carlo Serpent2 (ver. 2.1.24) code [7] was used to generate the 2-group constants of the target pin cells from infinite fuel assembly (FA) lattice calculations and 2-D whole core calculation. A total of 5,000 cycles including 500 inactive cycles were simulated separately: 500,000 histories per cycle in the infinite lattice calculations and 3,000,000 histories per cycle in the 2-D whole core calculation, resulting in relative statistical errors of 10^{-5}~10^{-3} for the evaluated cross sections. Fully explicit models (fuel rods, clad, clad gap, coolant, etc.) were used in all simulations.

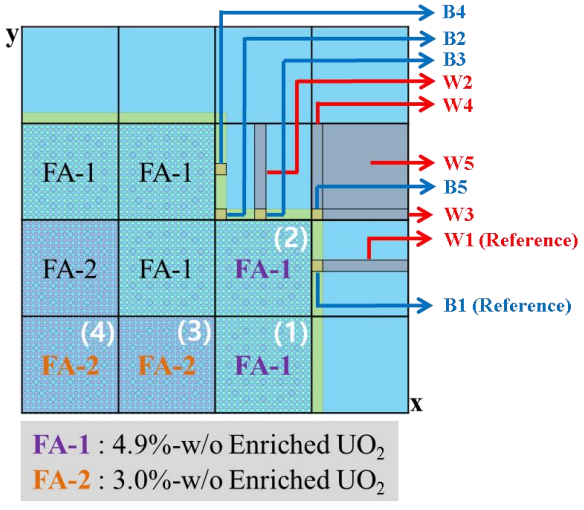

Fig. 1. The modified EPRI-9 benchmark problem

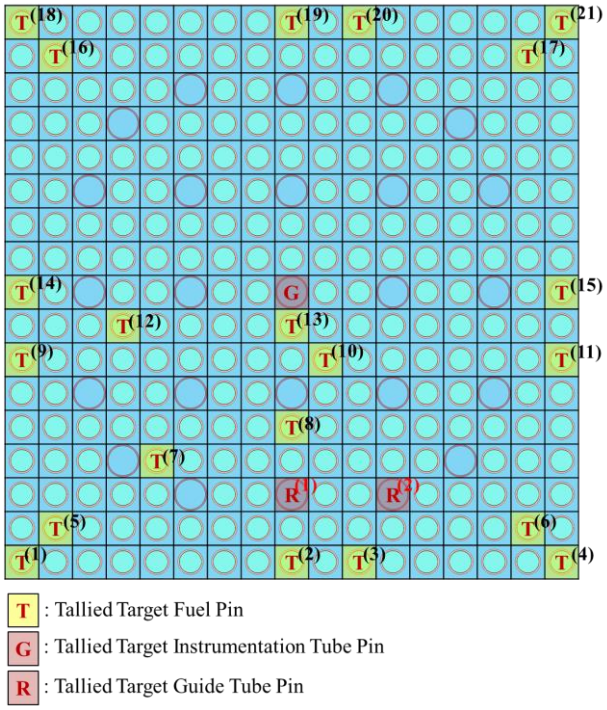

Fig. 2. Fuel assembly design with target pin cells for tally

Table I: Materials and temperatures modeled in the problem

Region	Material	Temperature (K)
Fuel	UO_2 (FA-1 3 w/o, FA-2 4.9 w/o)	800
Fuel gap	Helium	625
Fuel clad	ZIRLO	625
Coolant & reflector	Water (no boron)	600
Control rod (CR)	Ag-In-Cd (black rod)	
CR gap	Oxygen	
CR clad	SS304	
Guide thimble	ZIRLO	
Baffle	SS304	

In summary, two separate MC Serpent2 calculations were performed to tally the homogenized target pin cell 2-group constants: (1) infinite FA (reference data for the comparison) and (2) 2-D whore core calculations. These two calculations were subsequently compared to quantify effects of the pin environment on the 2-step pin-wise PWR core analysis.

2.2 Position-dependency of the 2-group Cross-sections

The 2-group homogenized pin cross sections (XS) determined using Serpent2's built-in functions are tabulated in Tables II and III according to its FA types and locations. It is clear that in FA-1 of position 1, where fuel pins and baffle are in contact (i.e., T4, T11, T15, and T21 pins), there are quite noticeable differences between the two sets of the homogenized 2-group constants. In fact, the fast-group errors are over 4.0% in the case of Σ_{abs}. This can be ascribed to the relatively softer neutron spectrum in the boundary layer neighboring the baffle-reflector region. The same phenomenon is observed at the same target pin cell in FA-1 of position 2. In addition, due to the L-shape baffle geometry in contact with the said FA, similar noticeable differences between the homogenized 2-group constants are also observed in target pin cells T18~T21. It is also noteworthy that the slowing down cross section is rather sensitive to the neutron spectrum, as expected.

Table II: Comparison of major cross sections for FA-1 (4.9 w/o enriched), Unit: cm^{-1}

Relative Error (%) in XS, FA-1 Position (1)							
Pin Position	Σ_{total}		Σ_{abs}		$\nu\Sigma_{fission}$		$\Sigma_{g1\to g2}$
	G1	G2	G1	G2	G1	G2	G1
T1	-0.46	0.90	-0.46	1.86	0.24	1.91	0.12
T2	-0.58	-0.01	-1.42	0.02	-1.06	0.02	-2.86
T3	-0.56	-0.05	-1.25	-0.01	-0.85	-0.01	-2.28
T4	0.98	-0.30	4.87	0.36	1.63	0.39	2.99
T5	-0.67	0.42	-1.20	0.97	-0.58	1.00	-1.47
T6	0.08	0.17	1.05	0.31	0.76	0.31	1.35
T7	-0.60	0.01	-1.41	0.09	-1.00	0.10	-2.64
T8	-0.59	-0.02	-1.62	0.01	-1.11	0.01	-2.81
T9	-0.48	0.90	-0.46	1.98	0.24	2.04	0.13
T10	-0.54	0.05	-1.19	-0.02	-1.03	-0.03	-2.58
T11	1.12	-0.42	4.76	0.13	1.55	0.15	3.33
T12	-0.66	0.10	-1.61	0.32	-1.07	0.33	-2.66
T13	-0.56	0.00	-1.40	0.02	-1.16	0.02	-2.39
T14	-0.45	0.90	-0.28	1.82	0.23	1.88	-0.11
T15	1.10	-0.44	4.92	-0.02	1.61	-0.01	2.83
T16	-0.59	0.28	-1.13	0.61	-0.59	0.62	-1.53
T17	0.09	0.14	0.95	0.22	0.74	0.22	1.34
T18	-0.46	0.56	-0.68	1.39	-0.23	1.44	-0.79
T19	-0.56	0.04	-1.40	0.09	-1.00	0.09	-2.77
T20	-0.61	0.01	-1.60	-0.10	-1.13	-0.10	-2.38
T21	1.03	-0.32	4.62	0.31	1.53	0.33	3.16
G	-0.58	0.00	-1.14	-0.03	_	_	-2.49
R1	-0.59	-0.04	-1.26	-0.04	_	_	-2.44
R2	-0.58	-0.01	-0.96	-0.01	_	_	-2.04
Relative Error (%) in XS, FA-1 Position (2)							
Pin Position	Σ_{total}		Σ_{abs}		$\nu\Sigma_{fission}$		$\Sigma_{g1\to g2}$
	G1	G2	G1	G2	G1	G2	G1
T1	-0.55	0.37	-1.15	0.65	-0.62	0.67	-1.56
T2	-0.55	-0.02	-1.46	-0.28	-1.16	-0.29	-2.72
T3	-0.60	0.01	-1.54	-0.23	-1.11	-0.24	-2.17
T4	1.05	-0.35	4.75	0.41	1.67	0.44	3.12
T5	-0.56	0.10	-1.41	0.17	-0.97	0.18	-2.37
T6	0.13	0.14	1.03	0.27	0.66	0.28	1.45
T7	-0.53	0.03	-1.38	0.06	-0.90	0.06	-2.59
T8	-0.57	-0.04	-1.50	0.02	-1.01	0.03	-2.52
T9	-0.51	-0.05	-1.45	0.09	-1.09	0.10	-2.75
T10	-0.51	0.04	-1.24	0.06	-0.97	0.06	-2.60
T11	1.11	-0.45	4.78	0.17	1.46	0.19	2.93
T12	-0.50	-0.03	-1.54	-0.02	-1.10	-0.02	-2.50
T13	-0.57	-0.05	-1.57	0.10	-1.04	0.11	-2.54
T14	-0.52	-0.06	-1.40	0.04	-1.00	0.05	-2.72
T15	1.15	-0.48	5.14	0.10	1.78	0.13	2.83
T16	0.38	-0.27	0.50	-0.46	-0.31	-0.47	-0.08
T17	0.38	0.65	2.86	1.24	2.29	1.26	4.66
T18	0.87	-1.33	2.36	-2.02	-0.56	-2.07	-0.60
T19	1.33	-0.19	5.15	0.44	1.26	0.47	3.09
T20	1.14	-0.15	4.73	0.75	1.16	0.78	2.99
T21	1.67	0.31	9.43	2.49	3.93	2.58	6.84
G	-0.51	-0.02	-0.74	-0.06	_	_	-2.25
R1	-0.59	-0.01	-1.90	-0.02	_	_	-2.59
R2	-0.55	0.01	-1.24	0.00	_	_	-1.94

Table III: Comparison of major cross sections for FA-2 (3.0 w/o enriched), Unit: cm^{-1}

Relative Error (%) in XS, FA-2 Position (3)							
Pin Position	Σ_{total}		Σ_{abs}		$\nu\Sigma_{fission}$		$\Sigma_{g1\to g2}$
	G1	G2	G1	G2	G1	G2	G1
T1	-0.18	-0.01	-0.53	0.05	-0.31	0.05	-1.10
T2	-0.17	0.01	-0.26	-0.14	-0.25	-0.15	-0.94
T3	-0.16	-0.04	-0.48	-0.08	-0.19	-0.08	-1.06
T4	-0.35	-0.67	-1.42	-1.49	-1.35	-1.54	-3.71
T5	-0.19	-0.01	-0.45	0.01	-0.21	0.02	-1.20
T6	-0.14	-0.28	-0.66	-0.72	-0.75	-0.75	-2.23
T7	-0.19	-0.01	-0.41	-0.09	-0.31	-0.10	-0.98
T8	-0.16	0.00	-0.47	-0.10	-0.33	-0.11	-0.94
T9	-0.16	-0.02	-0.56	-0.16	-0.38	-0.17	-0.84
T10	-0.15	-0.01	-0.39	-0.02	-0.26	-0.01	-0.88
T11	-0.38	-0.64	-1.44	-1.51	-1.34	-1.57	-3.52
T12	-0.17	0.00	-0.48	-0.09	-0.24	-0.10	-0.81
T13	-0.14	-0.01	-0.45	0.03	-0.31	0.04	-0.66
T14	-0.20	-0.02	-0.38	-0.05	-0.25	-0.05	-0.88
T15	-0.34	-0.68	-1.33	-1.44	-1.40	-1.49	-3.39
T16	-0.18	-0.25	-0.74	-0.62	-0.76	-0.65	-2.14
T17	-0.11	-0.54	-0.92	-1.26	-1.19	-1.31	-3.29
T18	-0.34	-0.46	-1.18	-0.90	-1.03	-0.92	-2.95
T19	-0.36	-0.70	-1.35	-1.53	-1.39	-1.59	-3.70
T20	-0.37	-0.65	-1.42	-1.50	-1.46	-1.56	-3.52
T21	-0.48	-1.19	-2.12	-2.59	-2.06	-2.69	-5.20
G	-0.16	0.01	-0.34	0.00	_	_	-0.73
R1	-0.14	-0.03	-0.46	-0.03	_	_	-0.69
R2	-0.12	-0.03	-0.31	-0.06	_	_	-0.66
Relative Error (%) in XS, FA-2 Position (4)							
Pin Position	Σ_{total}		Σ_{abs}		$\nu\Sigma_{fission}$		$\Sigma_{g1\to g2}$
	G1	G2	G1	G2	G1	G2	G1
T1	-0.18	-0.01	-0.42	-0.01	-0.26	-0.01	-1.09
T2	-0.18	-0.02	-0.42	-0.05	-0.21	-0.06	-0.94
T3	-0.19	-0.03	-0.34	-0.04	-0.28	-0.04	-0.96
T4	-0.19	0.02	-0.48	0.00	-0.28	0.00	-1.01
T5	-0.16	-0.01	-0.30	-0.01	-0.18	-0.01	-0.85
T6	-0.20	0.02	-0.46	-0.02	-0.24	-0.02	-1.10
T7	-0.19	-0.02	-0.50	-0.02	-0.32	-0.02	-0.85
T8	-0.17	-0.01	-0.40	0.00	-0.35	0.01	-0.89
T9	-0.19	0.02	-0.44	-0.03	-0.27	-0.03	-1.05
T10	-0.21	-0.05	-0.56	0.00	-0.35	0.00	-0.85
T11	-0.19	0.02	-0.44	-0.22	-0.33	-0.24	-1.00
T12	-0.20	0.02	-0.59	-0.06	-0.33	-0.07	-0.73
T13	-0.19	-0.02	-0.57	0.04	-0.36	0.04	-0.91
T14	-0.18	0.01	-0.45	-0.04	-0.23	-0.04	-0.96
T15	-0.17	-0.02	-0.34	-0.04	-0.17	-0.04	-0.83
T16	-0.20	-0.01	-0.42	-0.04	-0.17	-0.04	-0.90
T17	-0.11	-0.11	-0.44	-0.20	-0.49	-0.21	-1.26
T18	-0.18	0.01	-0.40	0.01	-0.27	0.01	-1.10
T19	-0.17	0.00	-0.49	-0.08	-0.37	-0.08	-0.99
T20	-0.16	-0.01	-0.57	-0.05	-0.39	-0.05	-0.84
T21	-0.22	-0.24	-0.87	-0.55	-0.76	-0.57	-2.04
G	-0.21	0.00	-0.50	-0.01	_	_	-1.07
R1	-0.17	-0.04	-0.71	-0.05	_	_	-0.84
R2	-0.19	0.01	-0.26	0.00	_	_	-0.85

The fuel pins can be grouped according to its pin environment depending on its relative position in the assembly. For instance, in FA-1 of position 2, T4, T11, T15, T19, and T20 pin cells can be grouped together as they border a similarly flat baffle-reflector region, resulting in similar XS discrepancies. T21 (corner pin) is not included in the above group since it is actually in contact with L-shape baffle-reflector region, which subsequently leads to the biggest XS discrepancies of all 21 target pin cells. One notes that T17 is significantly affected by T21 since T21 is located in the immediate 3x3 pin neighborhood of T17. Therefore, XS errors of T17 closely imitate discrepancy trend of T21. Furthermore, corner pin T18 is also not included in the aforementioned group since it has one extra fuel pin in its 3x3 pin neighborhood domain.

The fuel pins T7, T8, T10, T12, and T13 which are located in the central south-west quadrant of the FA can be grouped together since they have similar 3x3 pin neighborhood (1 or 2 GT in the domain). It is observed that T7 and T8 show almost identical XS errors albeit T7 has two GTs in its 3x3 pin neighborhood while T8 has one only. There are two main reasons for this observation: (1) GTs are uniformly distributed inside FA such that most fuel pins inside the 17x17 FAs have at least one GT in its 3x3 pin domain, and (2) mean free paths of fast and thermal neutrons are ~150% and ~70% of the pin pitch respectively; i.e. the fuel pins are tightly coupled in the domain. Therefore, the impact of adding one more GT in the neighborhood domain is not as strong as one would expect.

In the case of GTs G, R1, and R2 for both types of FA, they are all positioned on the inside of the FA and surrounded by the same number of fuel pins. Therefore, their XS errors are very similar depending on the FA.

Patterns of relative errors in FA-2 of positions 3 and 4 can also explained by the above observations. In general, errors in FA-2 are smaller than those of FA-1 because FA-2s are positioned in the interior region of the core. In other words, they are less affected by the very different baffle-reflector spectrum.

Position-dependency of baffle and reflector XS was also quantified in this work. The target baffle squares (labeled B1 to B5 of 2x2 pin size) and reflector slabs (labeled W1 to W4 of 15x2 pin size, and W5 of 15x15 pin size) are shown in Figure 1. All homogenized XSs of the target baffles and reflectors were generated using the MC Serpent2 code from the 2-D whole core calculation. B1 and W1 regions were chosen as baseline for XS comparison because they are the closest to typical 1-D spectral geometry model for a baffle-reflector simulation. The results are tabulated in Tables IV and V. One important observation from this comparison is that the absorption and down-scattering XSs of corner baffles (B2 and B5) show relatively bad agreement with those of flat baffle (B1). In fact, there is a sudden jump in fast-group absorption XS in W5. The strong position-dependency of the baffle and reflector cross sections is due to the significant neutron spectral differences between the regions.

Table IV: Comparison of major cross sections for baffle
Unit: cm^{-1}

Generated Baffle XS at Reference position					
Pin Position	Σ_{total}		Σ_{abs}		$\Sigma_{g1\to g2}$
	G1	G2	G1	G2	G1
B1	5.2953E-01	9.7836E-01	4.2232E-03	1.2930E-01	1.2067E-03
Relative Error (%) in XS					
Pin Position	Σ_{total}		Σ_{abs}		$\Sigma_{g1\to g2}$
	G1	G2	G1	G2	G1
B2	-0.47	-1.36	-6.34	-9.6	-12.05
B3	0.42	0.1	1.54	0.7	3.3
B4	0.44	0.1	1.51	0.67	2.8
B5	-0.31	0.82	5.86	5.8	12.49

Table V: Comparison of major cross sections for reflector, Unit: cm^{-1}

Generated Reflector XS at Reference position					
Pin Position	Σ_{total}		Σ_{abs}		$\Sigma_{g1\to g2}$
	G1	G2	G1	G2	G1
W1	6.5937E-01	1.7766E+00	3.3591E-04	8.9112E-03	4.1208E-02
Relative Error (%) in XS					
Pin Position	Σ_{total}		Σ_{abs}		$\Sigma_{g1\to g2}$
	G1	G2	G1	G2	G1
W2	1.69	0.03	3.92	0.05	6.35
W3	-0.04	0.17	2.66	0.28	2.22
W4	-0.42	0.32	4.76	0.54	3.58
W5	-2.73	0.52	10.69	0.87	4.54

3. Conclusions

In this study, position-dependency of the fuel pin homogenized cross sections in a small PWR core has been quantified via comparison of infinite FA and 2-D whole core calculations with the use of high-fidelity MC simulations. It is found that the pin environmental affect is especially obvious in FAs bordering the baffle-reflector regions. It is also noted that the down-scattering cross section is rather sensitive to the spectrum changes of the pins. It is expected that the pin-wise homogenized cross sections need to be corrected somehow for accurate pin-by-pin core calculations in the peripheral region of the reactor core.

The impact of pin homogenized cross sections position-dependency will be further studied by comparing its core multiplication factor and pin power distribution against those evaluated using the high-fidelity fully explicit whole core transport calculation and the conventional 2-step reactor analysis procedure.

REFERENCES

[1] José J. Herrero, Nuria García-Herranz, Diana Cuervo, Carol Ahnert, "Neighborhood-corrected interface discontinuity factors for multi-group pin-by-pin diffusion calculations for LWR," *Annals of Nuclear Energy*, 46, pp. 106-115, 2012

[2] S. H. Song, H. Y. Yu, and Y. Kim, "An Efficient One-Node and Two-Node Hybird CMFD Method for Pin-by-Pin Reactor Analysis," *Proceedings of Korean Nuclear Society Autumn Meeting*, Gyeongju, Korea, October, 2015.

[3] K. S. Smith, "Spatial Homogenization Techniques for Light Water Reactor Analysis," *Prog. Nucl. Energy*, Vol. 17, No. 3, pp. 303-335, 1986

[4] A. Hébert, "A Consistent Technique for the Pin-by-Pin Homogenization of a Pressurized Water Reactor Assembly," *Nuclear Science and Engineering*, 113, pp. 227-238, 1993

[5] H.S. Khalil, "The Application of Nodal Methods to PWR Analysis", Ph.D. Thesis, Department of Nuclear Engineering, Massachusetts Institute of Technology, Cambridge, MA, 1983.

[6] Public Version of AP1000 Design Control Document Revision 19, Westinghouse Electric, USA, 2011.

[7] Leppanen, J., 2012. Serpent user's manual. http://www.montecarlo.vtt.fi